Research Article

Yossra Ahmed Trabik*, Reham Abd El-Aziz Ismail*, Miriam Farid Ayad, Lobna Abd El-Aziz Hussein, and Amr Mohamed Mahmoud*

Microfabricated potentiometric sensor based on a carbon nanotube transducer layer for selective Bosentan determination

https://doi.org/10.1515/revac-2023-0071
received August 02, 2023; accepted January 04, 2024

Abstract: In this work, a solid-state electrochemical sensor relying on potentiometric transduction was constructed and optimized to detect Bosentan (BOS) in its pharmaceutical dosage form and human plasma. BOS is useful in pulmonary hypertension management as a nonselective endothelin receptor antagonist. A printed circuit board has been constructed and used as a substrate for microfabricated Cu electrodes. In comparison to a microfabricated control (Cu/ISM) electrode, the sensor potential signal drift was enhanced, and the response time was reduced by using multiwalled carbon nanotubes (MWCNTs) as an ion-to-electron transducer layer. According to IUPAC requirements, the suggested BOS sensors have been electrochemically characterized, and the linear dynamic range is (1.0×10^{-8} to 1.0×10^{-5}) M with a limit of detection of 6.28×10^{-9} M and 6.12×10^{-9} M for MWCNT-based sensor (Cu/CNT-NC/ISM) and control sensor (Cu/ISM), respectively. The described sensors have been used successfully to selectively determine BOS in dosage form and human plasma without any pre-treatment steps.

Keywords: Bosentan, microfabricated sensors, solid-contact electrodes, carbon nanotubes, ion-to-electron transducer

*** Corresponding author: Yossra Ahmed Trabik,** Pharmaceutical Analytical Chemistry Department, Faculty of Pharmacy, Ain Shams University, Organization of African Unity Street, Abassia 11566, Cairo, Egypt, e-mail: ytrabik@pharma.asu.edu.eg
*** Corresponding author: Reham Abd El-Aziz Ismail,** Pharmaceutical Analytical Chemistry Department, Faculty of Pharmacy, Ain Shams University, Organization of African Unity Street, Abassia 11566, Cairo, Egypt, e-mail: rihamabdelaziz.ismail@pharma.asu.edu.eg
*** Corresponding author: Amr Mohamed Mahmoud,** Analytical Chemistry Department, Faculty of Pharmacy, Cairo University, El-Kasr El-Aini Street, 11562 Cairo, Egypt, e-mail: amr.bekhet@pharma.cu.edu.eg
Miriam Farid Ayad, Lobna Abd El-Aziz Hussein: Pharmaceutical Analytical Chemistry Department, Faculty of Pharmacy, Ain Shams University, Organization of African Unity Street, Abassia 11566, Cairo, Egypt

1 Introduction

Over 100 million people are thought to be affected by the lethal condition known as pulmonary hypertension (PAH), which has several different etiologies. A mean pulmonary artery pressure (mPAP) of 25 mmHg or higher at rest is used to haemodynamically identify this disease, which can have major complications such as heart failure. Endothelin receptor antagonists, such as Bosentan (BOS), are an important class of drugs that have a role in the management of PAH [1]. BOS (4-*tert*-butyl-*N*-[6-(2-hydroxyethoxy)-5-(2-methoxyphenoxy)-2-(pyrimidin-2-yl)pyrimidin-4-yl] benzenesulphonamide) (Figure 1), is an oral antagonist of endothelin A and B receptor. High amounts of endothelin, which is a potent blood vessel constrictor, have been found in plasma and lung tissue of individuals with PAH. In 2001, the US Food and Drug Administration granted BOS, as the first orally active drug, license for the treatment of PAH. Through vasodilation, antifibrotic and antithrombotic actions, it relieves symptoms, notably in people with World Health Organization Class III or IV symptoms [2–4]. Another potential medical use for BOS is that it could also be used, in combination with other approved drugs, in the remediation of COVID-19 due to its antiviral effects [5,6]. In order to determine BOS in pharmaceutical dosage forms and biological fluids, many analytical techniques such as chromatography and spectroscopy have been published. However, to the best of our knowledge, no potentiometric assay has been reported for BOS determination [7–11]. Potentiometric approach has many advantages over other methods for sample analysis. These include fast response time, broad linear range, low energy and cost, simplicity of preparation, good sensitivity, and selectivity for many samples. In addition, potentiometric approaches do not need pre-treatment steps or the use of organic solvents, which makes them more eco-friendly. Other methods, on the other hand, are not appropriate for large-scale monitoring due to their high cost, complex usage, high energy and time consumption, and sample

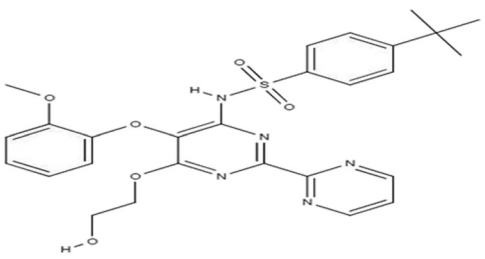

Figure 1: Chemical structure of BOS (drawn by chemibio draw ultra).

pre-treatment requirements. Therefore, potentiometric assay is a better option for sample analysis [12]. Potentiometric ion sensors are essential members of the family of electrochemical sensors that can electrochemically measure primary ion activity in a variety of sample matrices with minimal sample pre-treatment [13–16]. A new generation of ion-selective electrodes was developed: solid-contact ion-selective electrodes (SC-ISEs), which, among other benefits, were able to prevent internal filling solution leakage that occurred in the traditional liquid ion-selective electrodes [17,18]. As a result of the quick development of micro/nanofabrication processes and upraised understanding of concepts and techniques of electrochemistry, micro/nanoelectrode array sensing has recently withdrawn a lot of attention, particularly in the field of bioanalysis [19]. Recently, it has been verified that nanoparticles are valuable additions that enhance ion-selective electrode performance and minimize electrical resistance [20,21]. Using copper microfabricated electrodes to create SC-ISEs has the advantages of both microfabrication and SC-ISEs, such as low cost, miniaturization, simplicity, portability, real-time analysis, energy savings, the ability to be applied on large-scale analysis, robustness, and reliability [13,22,23]. This study aimed to develop a potentiometric sensor in order to determine BOS in human plasma and its dosage forms while complying with green analytical chemistry (GAC) through the fabrication of microfabricated copper solid contact-based potentiometric electrodes. The designed sensor response was improved to minimize signal drift and long response time via modification using carbon nanotubes (CNTs) as an ion-to-electron transducer interlayer. Because of CNTs' spacious nominated surface area and premium chemical stability, these CNT-based SC-ISEs have elevated potential stability and helped in improving SC-ISEs performance. To examine the importance of the transducer layer, the water layer test and signal drift were studied. Green Analytical Procedure Index (GAPI), Analytical Eco-Scale Green, and Analytical GREEnness Metric Approach and Software (AGREE) were used to assess the greenness of the suggested approach.

2 Experimental

2.1 Materials and reagents

BOS (purity 99.99%) was donated by EVA Pharma (Cairo, Egypt). Ambrisentan (AMB) (purity 99.99%) was endowed by AUG Pharma (Cairo, Egypt). Tridodecylmethylammonium chloride as an anionic exchanger was bought from Sigma-Aldrich (Cairo, Egypt). Polyvinyl chloride (PVC) was purchased from Fluka (Seelze, Germany). Tetrahydrofuran (THF) was obtained from Qualikems Fine Chem Pvt Ltd (Delhi, India). Dioctyl phthalate (DOP) was obtained from Acros Organics (Morris Plains, NJ, USA) and multi-walled carbon nanotubes (MWCNTs) from Sigma-Aldrich (Cairo, Egypt). Glacial acetic acid, acetone, sodium hydroxide (NaOH), and ammonium persulphate ($NH_4S_2O_8$) were purchased from El Nasr Company (Cairo, Egypt). Samples of human plasma were acquired from VACSERA (Giza, Egypt) and kept at −4°C. Pulmiprove® 62.5 mg tablet was obtained from a community pharmacy. Printed circuit boards (PCBs) with photoresist coating were acquired from the local market.

2.2 Standard solutions

2.2.1 Stock BOS standard solution

A stock solution of BOS (1.0×10^{-5} M) was made by weighing 1.5 mg of BOS into a 250 mL volumetric flask, which was then dissolved in an adequate quantity of carbonate buffer (pH = 9.2) before filling up to the final volume using the same buffer.

2.2.2 Working BOS standard solutions

Freshly made solutions of various strengths (1.0×10^{-6} –1.0×10^{-10} M) were made by successive dilutions from stock solution using a carbonate buffer with a pH of 9.2.

2.3 Procedures

2.3.1 Microfabricated copper electrode preparation

In this study, a microfabricated copper electrode was used as a solid-contact electrode substrate. The electrodes were created in accordance with published instructions [18,23].

Using high-resolution laser printing equipment, CAD software was utilized to create a photomask, which was printed on a transparent sheet. The photomask on top of pre-sensitized photoresist-coated PCBs was subjected to UV light (365 nm) for 90 s, blocking the light away from the needed areas while excluding areas that were not covered. For removal of the exposed portion of the photoresist, 0.25 M NaOH was used (as a developer). The exposed Cu was wet etched at 40°C with 1.1 M $NH_4S_2O_8$. Acetone was used for stripping the photoresist and revealing the patterned Cu electrodes. The electrodes were first rinsed with water and then dipped in acetic acid to eliminate surface oxides just before applying either CNTs or an ion-selective membrane (ISM).

2.3.2 ISM preparation

The ISM was prepared by blending 190 mg PVC, 0.4 mL DOP, and 10 mg tridodecylmethylammonium chloride in 6.0 mL of THF.

2.3.3 Carbon nanotubes/PVC nanocomposite preparation

The solution-blending method was used to prepare CNTs/PVC nanocomposite (CNT-NC), as described in the literature [24]. About 3.0 mL of THF and 0.2 mL of DOP were used to dissolve 95.0 mg PVC entirely. To obtain a homogeneous CNT-NC dispersion, MWCNT (10 mg) was mixed with the above-mentioned solution in an ultrasonic bath to ensure proper dispersion of nanomaterials in THF.

2.3.4 Solid-state ion-selective electrode fabrication

The microfabricated potentiometric sensor 1 (Cu/CNT-NC/ISM) was developed by applying 10.0 µL of CNT-NC dispersion onto the Cu microfabricated electrode and leaving it 24 h for solvent evaporation. Then, 10.0 µL of the ion-sensing cocktail was applied to the copper-modified electrode as presented in Scheme 1 and allowed to dry overnight. As a preconditioning phase, the sensor was immersed in a 1.0×10^{-5} M BOS solution for 1 day at 25°C before being used for the first time. CNT-NC free sensor as a control sensor (sensor 2, Cu/ISM) was prepared to examine the CNT-NC effect on potential drift and response time.

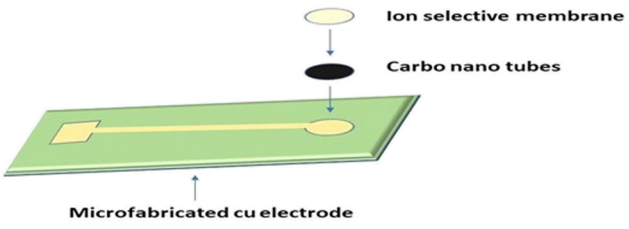

Scheme 1: A schematic illustration of a microfabricated solid-contact sensor 1.

2.3.5 Potentiometric measurements

Potentiometric experiments were performed using a Jenway pH meter 3310 Orion, reference electrode (Ag/AgCl, double junction) model. Bandelin Sonorox, Rx 510 S, and magnetic stirrer (Budapest, Hungary) as well as Jenway pH glass electrode (UK) were used for pH adjustment. Each sensor was individually coupled with an Ag/AgCl double junction reference electrode, calibrated by being submerged in BOS drug solutions (1.0×10^{-5}–1.0×10^{-10} M). Solutions were allowed to equilibrate till the potentiometer's readings were steady. The observed emf from the two suggested sensors was shown on calibration graphs in relation to – log [BOS] concentrations. Regression equations were computed for the suggested sensors. The sensors' performance was validated in conformity with IUPAC recommendations [25].

2.3.6 Sensor selectivity

A matched potential approach was used to evaluate the potentiometric selectivity factor. The change in potential (E) related to increased activity of the analyte from a_A = 1.0×10^{-8} M (reference solution) to a'_A = 1.0×10^{-5} M is recorded. Then, an interfering ion solution a_B with a concentration range of 5.0×10^{-8} –1.0×10^{-5} M is mixed with another 1.0×10^{-8} M (reference solution) until the same potential change (ΔE) is observed [26]. The next equation was used to determine the selectivity coefficient K for each interferent

$$K_{A,B}^{MPM} = \frac{a_A - a_A}{a_B}.$$

2.3.7 pH effect on sensor performance

Over a pH range of 3.0–11.0 regulated by adding 0.1 N HCl and 0.1 N NaOH, the impact of pH on the response of the studied sensors was observed on 1.0×10^{-6} M and 1.0×10^{-7} M BOS solutions. At each pH level, potential values were acquired and recorded.

2.3.8 Water layer test

The water layer test was developed by the Pretsch group [27–29]. It is used to determine whether a layer of water exists between the ion-to-electron transducer layer and the ISM. Potentiometric readings were acquired for 1.0×10^{-6} M BOS for 1 h; then, a more concentrated interfering solution (1.0×10^{-5} M AMB) was placed, and the potential was measured for another 1 h and returned to 1.0×10^{-6} M BOS for the third hour.

2.3.9 Analysis of BOS in pharmaceutical tablet formulation

Ten BOS tablets were precisely weighed, the tablet mean weight was determined, and the tablets were then pulverized. Of this powder, a precise quantity was weighed out, equal to 1.5 mg of BOS, then put into a 250 mL volumetric flask and diluted to the appropriate concentration with carbonate buffer, pH 9.2. The resultant solution was claimed to have a concentration of 1.0×10^{-5} M, then another two concentrations were prepared (1.0×10^{-6}, 1.0×10^{-7} M). Following Section 2.3.5, the measurements were carried out, and the recovery percentages were determined using the corresponding equations.

2.3.10 Analysis of BOS in spiked plasma

One millilitre of human plasma was put into a set of three volumetric flasks (10 mL); then, 1.0 mL, 550 µL, and 100 µL of BOS stock solution were added and completed to the final volume with carbonate buffer (pH 9.2) to prepare 1.0×10^{-6}, 5.5×10^{-7}, and 1.0×10^{-7} M. Following Section 2.3.5, the measurements were carried out, and the recovery percentages were determined using the corresponding equations.

3 Results and discussion

For analysts, building SC-ISEs with consistent and repeatable potentials has always been a big challenge. The aim of this study was the fabrication of portable, affordable, miniature-sized solid-contact sensors with highly sensitive, reproducible, and consistent readings.

3.1 Performance of the investigated sensors

Since BOS has a sulphonamide group (pK_a = 5.8) that carries a negative charge in a basic medium, this study was performed at an alkaline pH (9.2) [30]. The necessity of an anion exchange mechanism is required for BOS ion-selective electrode membranes; therefore, tridodecyl methyl ammonium chloride was used to introduce a lipophilic anionic exchanger, where the exchangeable counter ion (Cl^-) was initially replaced with BOS by conditioning the membrane for 1 day in 1.0×10^{-5} M BOS [31,32]. PVC was used as a polymer matrix in the fabrication of the ion-sensing cocktail. In this study, MWCNT-based sensor performance (sensor 1, Cu/CNT-NC/ISM) was evaluated compared to the control CNT-NC free sensor (sensor 2, Cu/ISM). According to IUPAC recommendations, the performance characteristics of the suggested sensors were assessed [25] and are listed in Table 1. The calibration plots' slopes for sensors 1 and 2 exhibited near-Nernstian response and were found to be 61.24 mV/concentration decades and 58.49 mV/concentration decades, respectively. The suggested sensors covered a dynamic linear concentration range of 1.0×10^{-5}–1.0×10^{-8} M, as shown in Figure 2. From the point where the two curves' linear extrapolated portions meet, the limit of detection (LOD) in accordance with IUPAC recommendations was determined and found to be 6.28×10^{-9} M for sensor 1 and 6.12×10^{-9} M for sensor 2 [25]. Short dynamic response time is a key parameter for increasing the number of samples that can be quickly analysed and hence contributes to the analytical application of the developed sensors [33]. For concentrations higher than 1.0×10^{-7}

Table 1: Performance characteristics of the investigated sensors for BOS determination

Parameter	Sensor 1	Sensor 2
Slope (mV/decade)[a] ± SD	61.24 ± 0.18	58.49 ± 0.35
Intercept (mV)[a] ± SD	114.14 ± 1.2	516.24 ± 2.1
Correlation coefficient (*r*)	0.9997	0.9998
Response time	31 s	1.37 min
Working pH range	7.5–10.5	7.5–10.5
Concentration range (M)	1.0×10^{-5}–1.0×10^{-8}	1.0×10^{-5}–1.0×10^{-8}
Stability (days)	30	23
Accuracy[a] (mean ± SD)	101.47 ± 1.10	101.26 ± 1.45
Precision (% RSD) Intra-day precision[b]	0.202	0.248
Inter-day precision[c]	0.499	0.479
LOD (M)[d]	6.28×10^{-9}	6.12×10^{-9}

[a] Average of three determinations.
[b] Intra-day precision (n = 9), an average of three different concentrations repeated three times within the same day.
[c] Inter-day precision (n = 9), an average of three different concentrations repeated on three successive days.
[d] Limit of detection (according to the IUPAC definition, measured by the intersection of the extrapolated arms of non-responsive and the Nernstian segments of the calibration plot).

M, sensor 1 responds quickly in 31 s, while sensor 2 takes 1.37 min. Meanwhile, a comparatively longer time is needed for more diluted concentrations to achieve a stable potential that is 56 s for Cu/CNT-NC/ISM sensor 1 and 1.50 min for Cu/ISM sensor 2. As expected, the lowest concentrations give the longest response times due to the longer time needed to attain equilibration. The shorter response time of sensor 1 is attributed to the presence of MWCNTs as a transducer layer, whereas the transduction behaviour of MWCNTs can be attributed to a high double-layer capacitance in the CNT's ion selective sensor. In contrast with conducting polymers, where the transduction mechanism is based on ion-exchange mechanisms and redox reactions, MWCNTs are more robust against any redox side reactions that might occur in the electrode [34]. The transducer layer (CNT) has been previously characterized using both Raman spectroscopy and SEM imaging techniques [35].

3.2 Monitoring of signal drift and water layer test

The sensor's response time and signal drift can both be affected by a water layer that might be formed between the electrode substrate and the ISM; hence, the water layer test was performed to detect its presence [27–29]. The test relies on spotting potential drift when switching between a primary ion solution (BOS; 1.0×10^{-6} M) and a potent interfering ion solution (AMB; 1.0×10^{-5} M), then switching back to the primary ion solution (BOS; 1.0×10^{-6} M). Although the control Cu/ISM (sensor 2) showed good potentiometric properties, it had a long response time (1.37 min) and observable drift (25 mV·h^{-1}), which is attributed to the formation of the water layer. In contrast to sensor 2, Cu/CNT-NC/ISM (sensor 1) had a lower response time (31 s) and less drift (1.9 mV·h^{-1}), as shown in Figure 3a and b, which is attributed to the hydrophobicity and high capacitance of CNTs that prevent the creation of a water layer between ISM in sensor 1 and the transducer layer.

3.3 pH effect on sensor response

To attain the optimum experimental conditions, the impact of pH on the effectiveness of the introduced sensors was evaluated. There was no noticeable change in the sensors' response in the pH range of 7.5–10.5, which is due to the presence of the sulphonamide group that has a negative charge in the basic medium. Below pH = 7.5, the drug began to precipitate, so the emf is no longer stable, as shown in Figure 4a and b.

3.4 Determination of sensors' selectivity coefficients

The selectivity of an ion-selective electrode is one of its most crucial features. It is frequently used to judge whether a valid measurement in the sample of interest is possible. Assessment of selectivity coefficients was done utilizing the matched potential method, which completely ignores the Nernst equation in order to circumvent the challenge of accurately determining selectivity coefficients in the presence of unequally charged ions [26]. Selectivity coefficients were assessed for structurally linked compounds such as AMB, co-administered drugs such as losartan and paracetamol, and other interfering ions such as chloride and citrate. Table 2 provides values for selectivity coefficients. The results revealed that both electrodes showed good selectivity towards BOS against other studied interferents. Sensor 1 (Cu/CNT-NC/ISM) showed relatively higher selectivity for

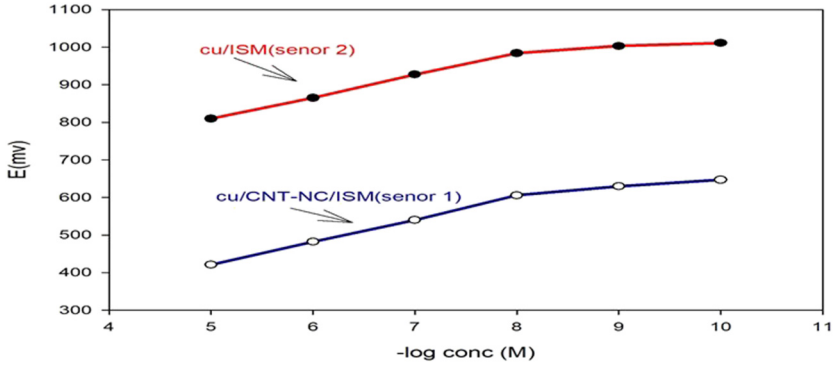

Figure 2: Profile of the proposed sensors' potential: (Cu/CNT-NC/ISM) sensor 1 and (Cu/ISM) sensor 2 in mV vs −log BOS (M) concentrations.

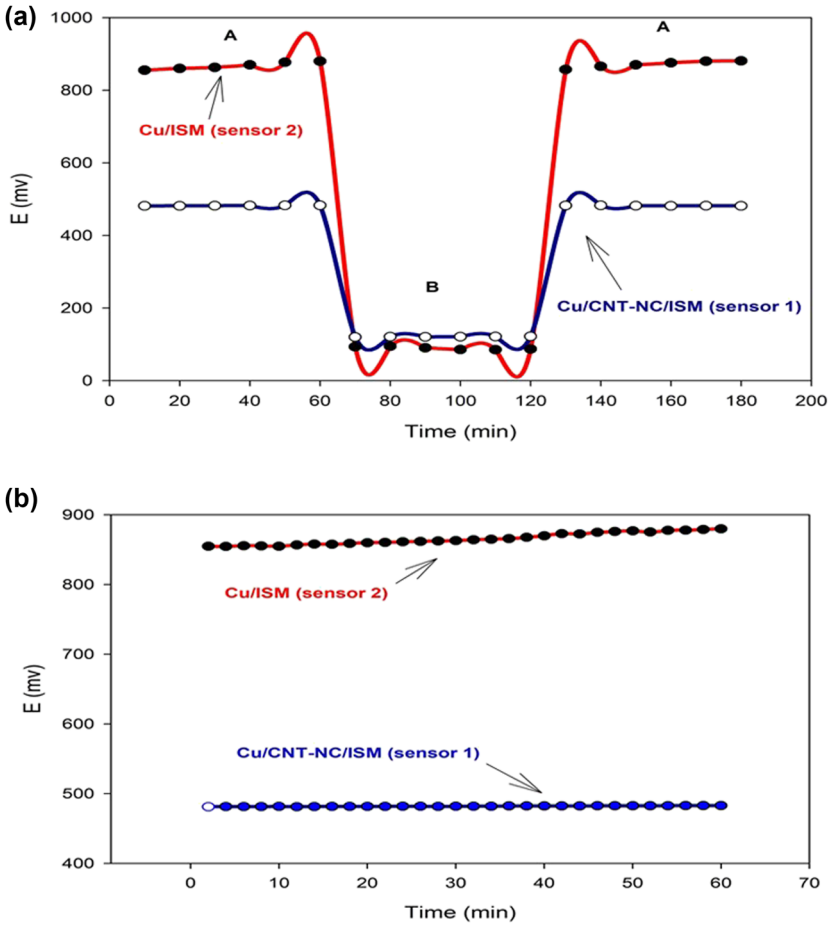

Figure 3: (a) Water layer test for sensors Cu/CNT-NC/ISM (sensor 1) and Cu/ISM (sensor 2). Measurements were recorded in 1.0×10^{-6} M BOS (a) and 1.0×10^{-5} M Ambrisentan (b). (b) Signal drift for Cu/CNT-NC/ISM (sensor 1) and Cu/ISM (sensor 2). Readings were recorded in 1.0×10^{-6} M BOS.

BOS in the presence of ambrisentan, losartan, citrate, and chloride ions than sensor 2 (Cu/ISM). In the presence of losartan, sensor 1 showed the highest selectivity for BOS, while the lowest selectivity was observed in the presence of paracetamol. As K^{MPM} BOS/interferent value decreases, it means that the sensor is more selective to the drug under study (BOS) [26].

3.5 Analysis of BOS in pharmaceutical tablet formulation

BOS in its pharmaceutical preparation (pulmivort tablets®) was directly measured without pre-treatment or extraction steps using the investigated sensors. As shown in Table 3, the suggested sensors were able to get precise and accurate recoveries. For the quantification of BOS in the formulation of pharmaceutical tablets, sensor 1 (Cu/CNT-NC/ISM) displayed the lowest SD values.

3.6 Analysis of BOS in spiked human plasma

$C_{\max}$ of BOS reaches a concentration of 1.12×10^{-6} M, after receiving a single 62.5 mg dose in healthy male volunteers on the first day [36]. This concentration is within the sensors' linear range. Thus, the proposed SC-ISE's ability to detect BOS in biological fluids was assessed using spiked human plasma directly with no preliminary treatment or extraction. The suggested sensors were successful in obtaining precise and accurate recoveries based on the data in Table 4. Sensor 1 (Cu/CNT-NC/ISM) showed a better recovery percentage than sensor 2 (Cu/ISM).

3.7 Greenness evaluation of the developed approach

The greenness of the developed approach was assessed using AGREE greenness assessment tools, GAPI, along with Analytical Eco-scale.

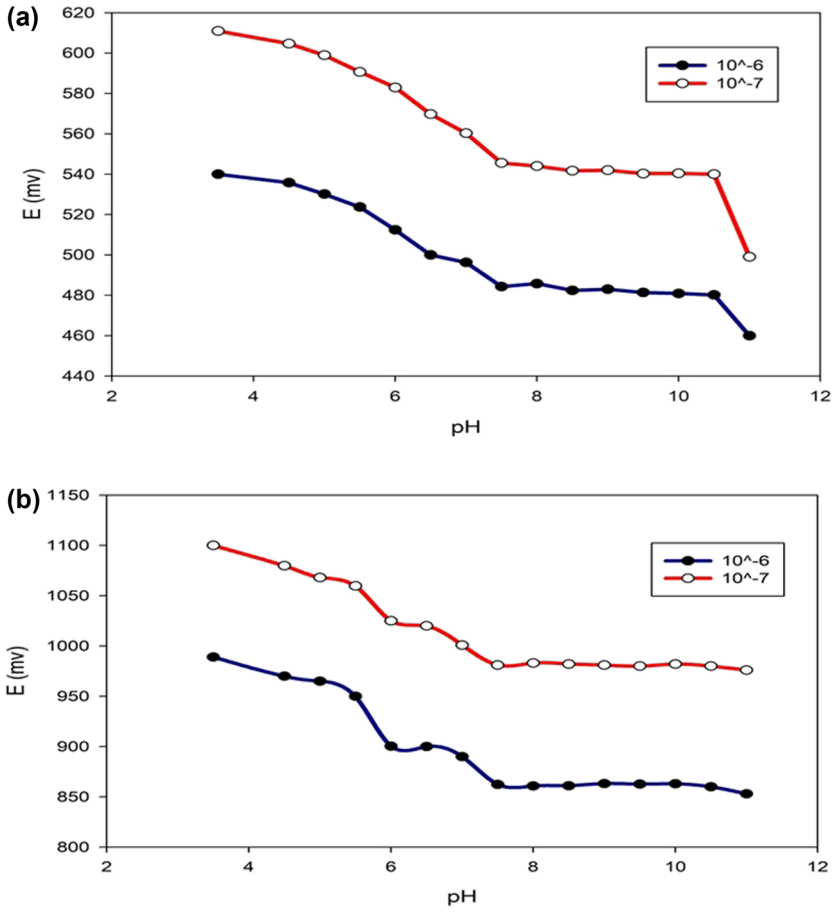

Figure 4: (a) pH effect on Cu/CNT-NC/ISM (sensor 1) response (working pH range: 3–11). (b) pH effect on Cu/ISM (sensor 2) response (working pH range: 3–11).

3.7.1 Analytical eco-scale

The analytical eco-scale [37] is calculated by deducting penalty points from a base of 100 for each analytical method component. In conformity with its standards, the method that is ideally green scores an eco-scale of 100, the excellent green method scores an eco-scale of more than 75, and the acceptable green method scores an eco-scale of more than 50 [38]. When the method yields an eco-scale score of less than 50, it is believed to be an inadequately green analytical method. The calculated penalty points for the suggested assay, revealing that the suggested approach has an excellent green Eco-Scale score, are illustrated in Table 5.

3.7.2 GAPI

The main benefit of GAPI is that it evaluates the greenness from sample collection till determination of its concentration,

Table 2: Potentiometric selectivity coefficients (K^{MPM} BOS/interferent) of the proposed sensors

Interfering element (I)	Sensor 1 K^{MPM} BOS/ interferent	Sensor 2 K^{MPM} BOS/ interferent
Ambrisentan	9.0×10^{-3}	1.6×10^{-2}
Losartan	1.8×10^{-3}	4.5×10^{-3}
Paracetamol	9.9×10^{-2}	8.2×10^{-2}
Citrate	9.8×10^{-3}	4.5×10^{-2}
Chloride	4.5×10^{-3}	8.2×10^{-3}

Table 3: Determination of BOS in pharmaceutical dosage form

Claimed concentration (M)	Recovery (%) ± % SD[a]	
	Sensor 1	Sensor 2
1.0×10^{-7}	100.73 ± 0.01	100.81 ± 0.74
1.0×10^{-6}	99.15 ± 0.20	98.13 ± 0.43
1.0×10^{-5}	101.8 ± 0.05	98. 92 ± 0.65

[a]Average of three determinations.

Table 4: Determination of BOS in spiked plasma

Spiked concentration (M)	Recovery (%) ± %SD[a]	
	Sensor 1	Sensor 2
1.0×10^{-6}	95.10 ± 0.41	92.84 ± 0.45
1.0×10^{-7}	94.60 ± 0.65	90.73 ± 0.52
5.5×10^{-7}	94.68 ± 0.75	92.82 ± 1.46

[a] Average of three determinations.

giving a comprehensive perspective of the suggested strategy [39]. Five pentagrams, each having a three-colour scale. Green indicates "low environmental impact," whereas yellow denotes "medium environmental impact," while red indicates "high environmental impact." Since there was no sample preparation step in this assay, its pentagram was eliminated. GAPI pentagram has green dominance, indicating that the procedure is of low risk, with only one yellow coloured part due to using THF during manufacture, and only one red coloured fraction denoting the total NFPA score of all the solvents. The GAPI pentagram is illustrated in Figure 5.

3.7.3 AGREE

Out of all the greenness evaluation techniques, only the AGREE approach uses all 12 GAC principles and yields an easily interpretable and informative result [40]. The analytical method is believed to be green for drug analysis if the AGREE analytical score are greater than 0.75. Additionally, a score of 0.50 indicates that the method is acceptable for drug analysis. Scores less than 0.50 show that the proposed analytical process is unacceptable. The proposed GAC electrodes in this work received an AGREE score of 0.78, as shown in Figure 6, indicating that the approach is extremely green and may be used safely in routine analysis.

Table 5: Penalty points for the greenness assessment of the proposed potentiometric approach

Hazard Reagents	Penalty points
Acetic acid (glacial)	4
acetone	4
Ammonium persulphate	6
Sodium hydroxide	2
PVC	1
THF	6
Instruments	
Energy (≤0.1 kW·h per sample)	0
Occupational hazard	0
Waste	0
Total penalty points	23
Analytical eco-scale total score	77

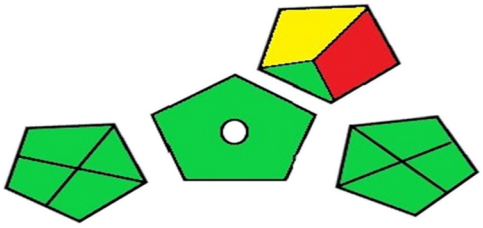

Figure 5: GAPI green profile assessment of the proposed method.

3.8 Statistical analysis

The variance ratio *F* test and Student's *t*-test were used to examine the validity of the proposed approach. A statistical comparison of the suggested sensors and the reported method [41] for BOS is presented in Table 6. The results show that there is no statistically significant difference between the reported method and the proposed sensors; the calculated *t* and *F* values were less than the theoretical ones at $p = 0.05$.

Figure 6: Results of AGREE green profile assessment software.

Table 6: Statistical comparison between the proposed assay and the reported reference method for the determination of BOS

Parameter	Reported method	Proposed assay	
		Sensor 1	Sensor 2
Mean	99.80	101.47	101.26
SD	0.45	1.10	1.45
Variance	0.20	1.21	2.12
N	3	4	4
Student *t*-test (2.571)		1.605	2.382
F (19.164)		5.937	10.407

Table 7: Comparison of other published analytical techniques for analysis of BOS

Technique	Matrix		Linear range (M)	LLOQ (M)	LOD (M)	Reference
HPLC-MS-MS	Human plasma		1.81×10^{-9}–1.81×10^{-5}	1.81×10^{-9}	—	[7]
HPLC-DAD	Tablet formulation		9.06×10^{-9}–1.27×10^{-7}	1.27×10^{-8}	3.63×10^{-9}	[11]
UV–VIS	Pharmaceutical dosage forms	A	3.63×10^{-6}–5.44×10^{-5}	2.36×10^{-7}	7.79×10^{-8}	[42]
		B	9.06×10^{-6}–5.44×10^{-5}	6.64×10^{-7}	2.19×10^{-7}	
		C	4.53×10^{-6}–9.06×10^{-5}	1.7×10^{-6}	5.6×10^{-7}	
HPLC-DAD		D	9.06×10^{-6}–1.81×10^{-4}	7.96×10^{-7}	2.62×10^{-7}	
UV–VIS spectrophotometer	Pharmaceutical dosage forms		1.8×10^{-7}–1.8×10^{-4}	1.8×10^{-7}	—	[9]
UV–VIS spectrophotometer	Human plasma		1.8×10^{-6}–9.07×10^{-6}	1.8×10^{-6}	1.27×10^{-7}	[10]
Linear sweep voltammetry	Pharmaceutical preparation		9.06×10^{-6}–7.25×10^{-5}	8.70×10^{-6}	2.90×10^{-6}	[43]
Square wave voltammetry			9.06×10^{-6}–6.35×10^{-5}	4.89×10^{-6}	1.63×10^{-6}	
Differential pulse voltammetry			9.06×10^{-6}–6.35×10^{-5}	1.63×10^{-6}	5.43×10^{-7}	
Microfabricated potentiometric sensors	Pharmaceutical tablet formulation-human plasma	1	1.0×10^{-8}–1.0×10^{-5}	—	6.28×10^{-9}	This work
		2	1.0×10^{-8}–1.0×10^{-5}	—	6.12×10^{-9}	

3.9 Comparison of other analytical techniques for analysis of BOS

Various techniques, including spectrophotometry, voltammetry, LC-MS, and HPLC, have been published for determining BOS and are summarized in Table 7. All these approaches, however, lack the mobility and affordability of the suggested potentiometric approach in addition to being slower and less straightforward compared to potentiometric analysis.

4 Conclusion

In this study, the described sensors were applied for the direct analysis of BOS in pharmaceutical formulation and human blood plasma. They showed many advantages over the traditional ion-selective electrodes in terms of stability and durability (30 and 23 days), as well as several advantages over other complicated methods such as HPLC, such as being eco-friendly, portable, a real-time analysis approach, easy to miniaturize, of low cost and energy saving. The proposed sensors demonstrated good, reproducible, accurate (a mean of 101.47 and 101.26 with SD < 2.0), precise (%RSD < 0.5), and selective potentiometric results in the presence of different interferents. They can be applicable for routine analysis without tedious pre-treatment procedures, due to their manufacturing simplicity and low cost. The addition of CNTs as an ion to electron transducer resulted in a shorter response time (31 s), lower signal drift, and almost no water layer is formed between the polymeric and transducer layers, as opposed to a blank ion-selective electrode free of ion to electron transducer, which had a longer response time (1.37 min) and a higher signal drift.

Acknowledgement: Sincere gratitude and appreciation are extended by the authors to EVA Pharma and AUG Pharma (Cairo, Egypt) for supplying gift samples of pure BOS and Ambrisentan. The authors would also like to thank Ain-Shams University's Department of Analytical Chemistry in the Faculty of Pharmacy for providing the tools and facilities needed to complete the research.

Funding information: Authors state no funding involved.

Author contributions: Yossra Ahmed Trabik: conceptualization, methodology, validation, investigation, writing – original draft, visualization. Reham Abd El-Aziz Ismail: conceptualization, methodology, validation, investigation, writing – original draft, visualization Miriam Farid Ayad:

conceptualization, methodology, validation, investigation, writing – original draft, visualization. Lobna Abd El-Aziz Hussein: conceptualization, methodology, validation, investigation, writing – original draft, visualization. Amr Mohamed Mahmoud: conceptualization, methodology, validation, investigation, writing – original draft, visualization.

Conflict of interest: Authors state no conflict of interest.

Data availability statement: The datasets generated during and/or analyzed during the current study are available from the corresponding author on reasonable request.

References

[1] Sysol JR, Machado RF. Classification and pathophysiology of pulmonary hypertension. Continuing Cardiol Educ. 2018 Jun;4(1):2–12.

[2] Lau EMT, Tamura Y, McGoon MD, Sitbon O. The 2015 ESC/ERS Guidelines for the diagnosis and treatment of pulmonary hypertension: A practical chronicle of progress. Eur Respir J. 2015;879–82.

[3] Hoeper MM, Kramm T, Wilkens H, Schulze C, Schäfers HJ, Welte T, et al. Bosentan therapy for inoperable chronic thromboembolic pulmonary hypertension. Chest. 2005 Oct;128(4):2363–7.

[4] Valerio CJ, Coghlan JG. Vascular Health and Risk Management Bosentan in the treatment of pulmonary arterial hypertension with the focus on the mildly symptomatic patient. Vasc Health Risk Manage. 2009 Aug;5:607–19.

[5] Shi Y, Wang Y, Shao C, Huang J, Gan J, Huang X, et al. COVID-19 infection: the perspectives on immune responses. Cell Death Differ. 2020;27(5):1451–4.

[6] Funke C, Farr M, Werner B, Dittmann S, Überla K, Piper C, et al. Antiviral effect of Bosentan and Valsartan during coxsackievirus B3 infection of human endothelial cells. J Gen Virology. 2010 Aug;91(8):1959–70.

[7] Lausecker B, Hess B, Fischer G, Mueller M, Hopfgartner G. Simultaneous determination of bosentan and its three major metabolites in various biological matrices and species using narrow bore liquid chromatography with ion spray tandem mass spectrometric detection. J Chromatogr B, Biomed Sci Appl. 2000;749(1):67–83.

[8] Dell D, Lausecker B, Hopfgartner G, Van Giersbergen PLM, Dingernanse J. Evolving bioanalytical methods for the cardiovascular drug bosentan. Chromatographia. 2002 Jan;55:115–9.

[9] Narendra A, Deepika D, Mathrusri Annapurna M. New spectrophotometric method for the determination of bosentan-An anti-hypertensive agent in pharmaceutical dosage forms. J Chem. 2012;9.

[10] Sajedi-Amin S, Assadpour-Zeynali K, Panahi-Azar V, Kebriaeezadeh A, Khoubnasabjafari M, Ansarin K, et al. Spectroscopic analysis of bosentan in biological samples after a liquid-liquid microextraction. BioImpacts. 2015 Dec;5(4):191–7.

[11] Muralidharan S, Kumar JR. Simple estimation of bosentan in tablet formulation by RP-HPLC. Am J Anal Chem. 2012;3(11):715–8.

[12] Isildak Ö, Özbek O. Application of potentiometric sensors in real samples. Critical Reviews in Analytical Chemistry. England: Taylor and Francis; Vol. 51, 2021; p. 218–31

[13] Shao Y, Ying Y, Ping J. Recent advances in solid-contact ion-selective electrodes: Functional materials, transduction mechanisms, and development trends. Chemical Society Reviews. Vol. 49; 2020. p. 4405–65.

[14] Bobacka J, Ivaska A, Lewenstam A. Potentiometric ion sensors. Chem Rev. 2008;108(2):329–51.

[15] Bakker E, Telting-Diaz M. Electrochemical sensors. Anal Chem. 2002;74(12):2781–800.

[16] Hussein LA, El-Kosasy AM, Trabik YA. Comparative study of normal, micro- & nano-sized iron oxide effect in potentiometric determination of fluconazole in biological fluids. RSC Adv. 2015;5(47):37957–63.

[17] El-Rahman MKA, Rezk MR, Mahmoud AM, Elghobashy MR. Design of a stable solid-contact ion-selective electrode based on polyaniline nanoparticles as ion-to-electron transducer for application in process analytical technology as a real-time analyzer. Sens Actuators B Chem. 2015 Mar 1;208:14–21.

[18] El-Mosallamy SS, Ahmed K, Daabees HG, Talaat W. A microfabricated potentiometric sensor for metoclopramide determination utilizing a graphene nanocomposite transducer layer. Anal Bioanal Chem. 2020 Nov 1;412(27):7505–14.

[19] Liu Y, Li X, Chen J, Yuan C. Micro/Nano Electrode Array Sensors: Advances in Fabrication and Emerging Applications in Bioanalysis. Frontiers in Chemistry. Front Media SA. 2020;8:573865.

[20] Ayad MF, Trabik YA, Abdelrahman MH, Fares NV, Magdy N. Potentiometric carbon quantum dots-based screen-printed arrays for nano-tracing gemifloxacin as a model fluoroquinolone implicated in antimicrobial resistance. Chemosensors. 2021;9(1):8.

[21] Trabik YA, Al-Afify NKH, El-Kosasy AM, Magdy N. Application of precipitation-based and nanoparticle-based techniques for fabrication of potentiometric sensors for nano molar determination of chitosan and polyvinyl pyrrolidone in pharmaceutical formulations and biological fluids. Electroanalysis. 2021 May;33(5):1233–43.

[22] Bakker E, Pretsch E. Modern potentiometry. Angew Chem – Int Ed. 2007;46:5660–8.

[23] Hassan SA, ElDin NB, Zaazaa HE, Moustafa AA, Mahmoud AM. Point-of-care diagnostics for drugs of abuse in biological fluids: application of a microfabricated disposable copper potentiometric sensor. Microchim Acta. 2020 Aug;187(9):491.

[24] Hasan M, Lee M. Enhancement of the thermo-mechanical properties and efficacy of mixing technique in the preparation of graphene/PVC nanocomposites compared to carbon nanotubes/PVC. Prog Nat Sci: Mater Int. 2014 Dec;24(6):579–87.

[25] Buck RP, Lindneri E. Recommendations for nomenclature of ion-selective electrodes. J Buffle Pure Appl Chem. 1994;66(12):2527–36.

[26] Umezawa', Yoshio, Kayoko Umezawa2 & Hitoshi Sat03. International union of pure and applied chemistry analytical chemistry division commission on electroanalytical chemistry * selectivity coefficients for methods for reporting k r b values ion-selective electrodes. Pure Appl Chem. 1995;67:507–18.

[27] Fibbioli M, Morf WE, Badertscher M, De Rooij NF, Pretsch E. Potential drifts of solid-contacted ion-selective electrodes due to zero-current ion fluxes through the sensor membrane. Electroanalysis. 2000;12(16):1286–92.

[28] Veder JP, de Marco R, Clarke G, Chester R, Nelson A, Prince K, et al. Elimination of undesirable water layers in solid-contact polymeric ion-selective electrodes. Anal Chem. 2008 Sep;80(17):6731–40.

[29] Hambly B, Guzinski M, Pendley B, Lindner E. Evaluation, pitfalls and recommendations for the "Water Layer Test" for solid contact ion-selective electrodes. Electroanalysis. 2020 Apr;32(4):781–91.

[30] Krupa A, Majda D, Mozgawa W, Szlęk J, Jachowicz R. Physicochemical properties of bosentan and selected PDE-5

inhibitors in the design of drugs for rare diseases. AAPS PharmSciTech. 2017 May;18(4):1318–31.
[31] El-Ragehy NA, Hegazy MA, AbdElHamid G, Tawfik SA. Validated potentiometric method for the determination of sulfacetamide sodium; application to its pharmaceutical formulations and spiked rabbit aqueous humor. Bull Fac Pharm Cairo Univ. 2018 Dec;56(2):207–12.
[32] Ragab MT, Abd El-Rahman MK, Ramadan NK, El-Ragehy NA, El-Zeany BA. Novel potentiometric application for the determination of pantoprazole sodium and itopride hydrochloride in their pure and combined dosage form. Talanta. 2015 Jun;138:28–35.
[33] El-Kosasy AM, El Aziz L, Trabik YA. Comparative study of beta cyclodextrin and calix-8-arene as ionophores in potentiometric ion-selective electrodes for sitagliptin phosphate. J Appl Pharm Sci. 2012 Aug;2(8):51–6.
[34] Crespo GA, Macho S, Rius FX. Ion-selective electrodes using carbon nanotubes as ion-to-electron transducers. Anal Chem. 2008 Feb;80(4):1316–22.
[35] Soliman RM, Rostom Y, Mahmoud AM, Fayez YM, Mostafa NM, Monir HH. Novel fabricated potentiometric sensors for selective determination of carbinoxamine with different greenness evaluation perspectives. Microchem J. 2023 Apr;187.
[36] van Giersbergen PL, Halabi A, Dingemanse J. Single- and multiple-dose pharmacokinetics of bosentan and its interaction with ketoconazole. Br J Clin Pharmacol. 2002;53(6):589–95.
[37] Gałuszka A, Migaszewski ZM, Konieczka P, Namieśnik J. Analytical Eco-Scale for assessing the greenness of analytical procedures. TrAC – Trends Anal Chem. 2012;37:61–72.
[38] Fahmy NM, Abdullatif HA, Michael AM, Ayad MF, Trabik YA. Smart Eco-friendly spectrophotometric methods resolving highly overlapping spectra: application to veterinary injections. J AOAC Int. 2022 Apr;105(5):1234–46.
[39] Płotka-Wasylka J. A new tool for the evaluation of the analytical procedure: Green Analytical Procedure Index. Talanta. 2018 May;181:204–9.
[40] Pena-Pereira F, Wojnowski W, Tobiszewski M. AGREE - Analytical GREEnness metric approach and software. Anal Chem. 2020 Jul;92(14):10076–82.
[41] Siddappa K, Hanamshetty PC. Development and validation of high performance liquid chromatography (HPLC) method for the determination of bosentan in pure and formulated forms. Der Pharmacia Lett. 2016;8:404–11.
[42] Lavudu PE, Rani AP, Sekaran CB, Ramesh A, Kumar A. Application of spectrophotometry and high performance liquid chromatography for the analysis of Bosentan in pharmaceutical dosage form. Chem Sci Trans. 2014 Oct;3(4):1242–53.
[43] Atila A, Yilmaz B. Determination of bosentan in pharmaceutical preparations by linear sweep, square wave and differential pulse voltammetry methods. Iran J Pharm Res. 2015;14(2):443–51.